The Production of a Liquid Fuel from Coke Oven By-product Gas and Biomass and the Establishment of a Method for the Use in advanced chemical applications

コークス副生ガス／バイオマスによる液体燃料化と化学原料化高度利用法の構築

Yukihiko Okumura, National Institute of Technology, Maizuru College

1. INTRODUCTION

Studies of the effective use of by-products and the effective use of waste energy in the steel making process are important for the advanced chemical applications and for the reduction of carbon dioxide retention. The present study examines two approaches to the intensive use of large amounts of by-product gas and by-product liquid as chemical raw materials in the coke production process. Some examples of by-product liquid-components obtained from coal are naphthalene, tar pitch, creosote oil, anthracene, phenol, and cresol [1]. These products are distinct from the chemical raw materials obtained from oil (organic synthetic chemical components) i.e., the products obtained from coals have unique chemical characteristics [2]. For example, rare components, such as indene and fluorene, are contained in coal tar (not found in oil). Indene is useful as a starting material for producing resin modifiers and medicines [3]. Optical properties including heat resistance and refractive index can be improved by incorporating indenes into resin. (Cardo structural skeleton incorporated orthogonal to the resin main chain.) By incorporating fluorene-skeleton into the resin, the following characteristics can be imparted to it [4]: compatibility between high refractive indices and low birefringence, heat resistance, high glass-transition point, and low dielectric constant. The aforementioned rare components are used to increase the functionality of resins such as polycarbonate, polyester, and polyimide. At present, more advanced applications of functional raw materials obtained from coal tar are constantly being studied.

In the present study, the effects of the heating rate and the coal type on the yields of useful by-product components are first examined to intensively use chemical raw materials (research objective-(1) in **Fig. 1**). In a national project of Japan, the heating rate in newly-built coke ovens is rapidly increased, in addition a large amount of non- or slightly-coking coal is mixed with caking coal in the SCOPE21 [5], (the Super Coke Oven for Productivity and Environmental Enhancement Toward the 21st Century). Since ~60% of other coal is replaced with conventional coal types [5], the composition of by-products may vary from the by-products obtained in the past. Multiple coal types have been used for coke, and the use of non-caking coal has steadily expanded

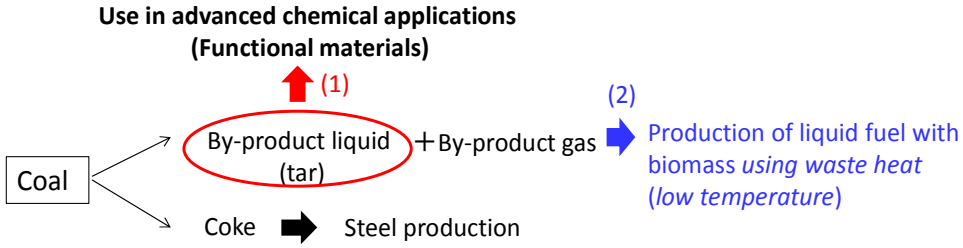

Fig. 1 Background and objectives ((1), (2))

for use in the future steel industry. Therefore, the effect of coal type on the yield of volatile matter (by-product liquid and gas components) must be elucidated. Although the yield of volatile matter is higher in fast pyrolysis than in slow pyrolysis [6],[7], no study has reported on the components and their increased or decreased amounts in detail. To achieve research objective-(1), we quantitatively investigated the effect of the heating rate on the yield of the volatile matter.

Next, as shown in research objective-(2) in **Fig. 1**, we propose a process in which the coke oven by-product gas is mixed with biomass, and a solid–gas reaction is facilitated at medium to low temperatures (in the temperature range of waste heat) to convert the mixture to CO and H_2. The technology of producing liquid fuel can contribute to the densification of fuel and the intensive use in automotive fuels and industrials. The addition of biochar is expected to facilitate the production of CO-rich gas ($C + CO_2 \rightarrow 2CO$) and provide the ideal CO/H_2 ratio for the Fischer-Tropsch (FT) synthesis. The methane gas can reform by the reaction ($CH_4 + H_2O = CO + 3\ H_2$) at medium temperature (in the temperature range of waste heat) using steam. Liquid fuel can be produced from the synthesized gas ($H_2 + CO$) obtained from the above reactions through dry refinement and the FT synthesis. The present study first examines a method to increase the gasification rate of biochar that determines the overall gasification rate. (The gasification rate of biochar is particularly important in a low-temperature range.) In summary, the present study elucidates the following two points:

(1) The gasification reaction rate represented by Arrhenius plot

(2) The enhancement of the char gasification reaction at low temperatures using a catalyst [Development of the constituent technology to facilitate gasification at low temperatures]

2. RESEARCH OBJECTIVE-(1)

[The Yield and Composition of By-product Gas and Liquid from Coal Pyrolysis]

2.1 Experimental Apparatus and Method

The thermogravimetric analyzer (**Fig. 2**: TGD9600, ALVAC) was used in this research objective-(1). A coal sample (**Table 1**, 100mg, under 100mesh) is placed in a platinum cell (height: 10mm, diameter: 8mm) in an argon atmosphere, and the coal is pyrolyzed by an infrared gold image furnace. When the maximum temperature of 1273 K is reached (ref. **Table 2**), the applied voltage is interrupted, thereby stopping the heating, and then the sample is abruptly cooled. Since radiation can pass unimpeded through Ar, the entrainment gas remains relatively cool and quenches the chemical reactions among the primary products as they are expelled.

The yields were defined as follows:

Total yield of volatile matter, $Y_{total\ V.M.}$:

$$Y_{total\ V.M.} = (M_{sample} - M_{char}) \ / \ M_{sample} \quad \cdots \quad (1)$$

Tar yield, Y_{tar}:

$$Y_{tar} = M_{tar} \ / \ M_{sample} \quad \cdots\cdots\cdots \quad (2)$$

M shows a weight, and M_{tar} is calculated from the change in the weight of the filter in the tar trap before and after each experiment.

Total yield of gas, $Y_{total\ gas}$:

$$Y_{total\ gas} = (M_{sample} - M_{char} - M_{tar}) \ / \ M_{sample} \quad \cdots \quad (3)$$

Here, the following equation holds:

$$Y_{total\ V.M.} = Y_{tar} + Y_{total\ gas} \quad \cdots\cdots\cdots \quad (4)$$

In case of the tar component analysis, the impingers (Figure 3) were used in stead of the tar trap in Figure 2. The tar is transported by the carrier gas Ar and collected by the impinger. The first layer of the impinger contains isopropyl alcohol solvent cooled by dry ice and the second layer contains acetone solvent cooled similarly (194.15K). In order to make the cooling process of the structure efficient, marbles (glass beads) were placed in the structure to increase the surface area of the bubbles formed.

For the tar-component analysis, a Shimadzu gas chromatograph–mass spectrometer (GCMS-QP2010 Ultra) was used. Rtx-5MS and helium were selected as the column and carrier gas, respectively. The temperature of the sample vaporization chamber was set at 280°C. The analysis was conducted by increasing the column oven temperature gradually as follows: 40°C (retention time: 5 min) -> temperature increase at 10°C/min -> 320°C (retention time: 5 min). This procedure was carried out in the high-precision control mode, in which the carrier gas was provided at a

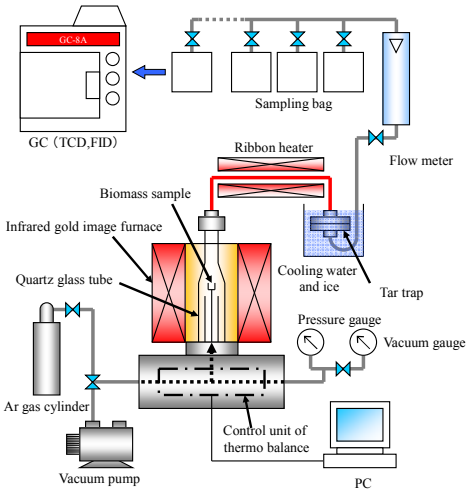

Fig.2 Outline of experimental apparatus

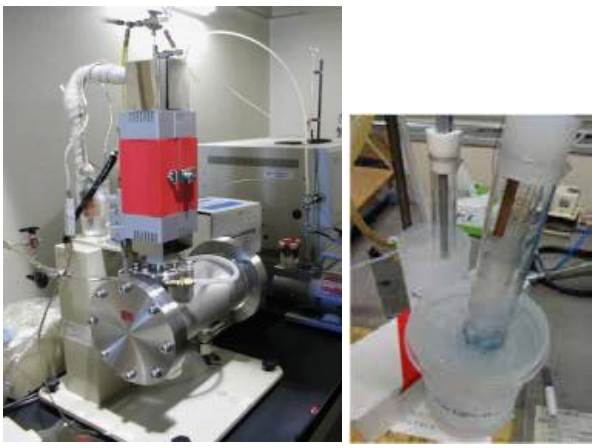

Fig.3 Experimental apparatus and impinger

Table 1 Coal properties

	Ultimate analysis(wt%, d.a.f.)					Proximate analysis (wt%)				Elemental composition	
	C	H	O	N	S	VM	FC	ASH	MOIST.	H/C	O/C
A-coal (SS011,IND)	73.1	5.1	20.8	1.0	0.0	40.65	45.19	1.58	12.58	0.837	0.213
B-coal (SS071, IDN)	76.2	5.4	16.0	1.8	0.53	39.87	45.02	5.81	9.30	0.850	0.157
C-coal(SS024, USA)	78.5	5.8	13.5	1.7	0.48	38.08	50.06	7.14	4.72	0.887	0.129
D-coal (SS002 , AUS)	81.2	6.1	10.6	1.6	0.58	38.04	45.20	14.52	2.24	0.901	0.098
E-coal (SS003, AUS)	82.9	4.7	10.2	1.8	0.31	28.44	60.00	8.56	3.00	0.680	0.092
F-coal (SS007, AUS)	83.8	5.3	8.9	1.3	0.66	31.60	51.10	15.00	2.30	0.759	0.080
G-coal (SS035, AUS)	88.3	5.1	4.5	1.6	0.48	18.33	65.93	14.54	1.20	0.693	0.038
H-coal (SS037, CHN)	90.6	4.2	3.4	1.3	0.4	8.49	73.40	16.54	1.57	0.556	0.028
(1)-coal (SS015 ,COL)	**80.7**	5.9	11.2	1.6	0.63	35.30	53.50	8.30	2.90	0.877	0.104
(2)-coal (SS027, CHN)	**80.6**	4.9	12.8	1.0	0.68	27.66	56.89	10.24	5.21	0.730	0.119
(3)-coal (SS028, AUS)	**80.8**	4.8	12.2	1.9	0.29	26.79	60.07	7.98	5.16	0.713	0.113
I-coal (SS048, AUS)	**84.0**	5.4	7.9	1.9	0.71	29.00	53.92	15.73	1.35	0.772	0.071
II-coal (SS022, ZAF)	**83.4**	4.8	9.2	2.0	0.61	26.40	57.09	13.73	2.78	0.690	0.083
III-coal (SS021, ZAF)	**84.4**	4.7	8.5	1.9	0.46	24.10	59.07	14.43	2.40	0.668	0.076
1-coal (SS050, AUS)	82.7	5.4	9.4	1.9	0.56	29.92	54.00	14.16	1.92	0.784	0.085
2-coal (SS058, CHN)	82.7	5.4	9.9	1.6	0.49	33.07	53.55	10.76	2.62	0.784	0.090
3-coal (SS036, AUS)	87.0	5.4	5.5	1.7	0.46	19.22	57.42	22.17	1.19	0.745	0.047
4-coal (SS064, CHN)	88.3	4.7	5.2	1.5	0.29	18.32	65.89	14.28	1.51	0.636	0.044
5-coal (SS067, CHN)	89.6	4.6	4.2	1.6	0.16	16.12	67.89	14.29	1.69	0.610	0.035

Table 2 Pyrolysis conditions

Atmospheric gas	Ar
Heating rate [K/s]	0.5 - 20.0
Maximum temperature [K]	1273
Holding time [s]	0.0
Pressure [MPa]	0.1 (1.0atm), 1.06

constant linear velocity (40 cm/s). Trial experiments were repeated to refine the peak separation, and the split ratio was determined to be 20. Fifty two types of tar components were quantified by using an internal standard method, which is considered to be the most accurate method. The calibration curve was prepared by using concentrations at three points; acetone was used as the solvent of the mixed standard samples. The quantities of the other 54 species of tar components were determined by using semiquantitative analysis based on the peak-area value of the total ion chromatogram (TIC) for Toluene-D8.

2.2 Experimental Results and Discussion

2.2.1 The composition and yield of pyrolysates generated during a rapid heating rate corresponding to that of SCOPE21

Figure 4 shows the volatile product yields of C-coal (see Table 1) as a representative example. The tar yield at atmospheric pressure increased with increasing heating rate, while the gas yield (obtained from $Y_{total\,gas} = Y_{total\,V.M.} - Y_{tar}$ in **Fig.4**) hardly changed. Under high pressure, $Y_{total\,V.M.}$ and Y_{tar} were suppressed. The total volatile matter yield exceeds the proximate analysis value, which is shown by the alternate long and short dashed lines in **Fig. 4**, at a heating rate of 5 K/s (P= 0.1MPa). The liquid color of the collected tar changed to dark-brown upon increasing the heating rate. (**Fig.5**)

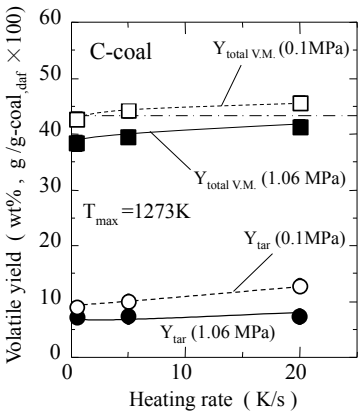

Fig.4 Effect of heating rate on first-pyrolysis yield

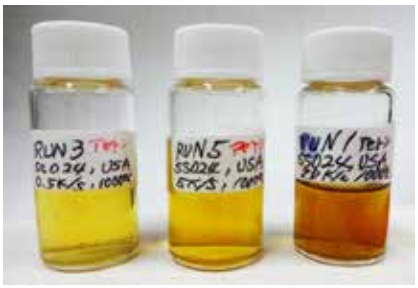

(a) 0.5K/s, (b) 5K/s, (c) 20K/s

Fig.5 Appearance of collected tar (1atm)

2.2.2 Effect of heating rate on tar component yield

Figure 6 shows the GC-MS chromatograms of the tar under the atmospheric pressure. The distinct high peaks of benzene, styrene, and indene are clearly observed on the left-hand side, and the peaks of heterocyclic tar components up to the 6-membered ring are observed on the right-hand side at 20K/s (**Fig.6(a)**). At a

slow heating rate, however, the chromatogram is composed chiefly of the peaks of tar with up to 4-membered rings (**Fig.6(b)**).

Figures 7 and **8** show the results of the detailed study of the tar components. Approximately 110 peaks with high intensities were analyzed to identify the chemical species involved. The analysis quantitatively specified the chemical species contained in 32 wt% of tar. (The chemical species contained in 43wt% of tar were identified by including semi-quantitative analyses.) **Figure 7** shows the detected number of only quantified chemical species, indicating that aromatic hydrocarbons of 1- to 2-membered-ring were formed in large numbers, while 5- to 6-membered ring components were formed in relatively small numbers. **Figure 8** shows the collected amounts of the tar species. The formation of benzene and toluene were much higher than that of other chemical species. The high-yield polycyclic aromatic hydrocarbon species with more than 3-membered rings were acenaphthene, phenanthrenea, and fluorene.

Figure 9 shows how the yield of each component varies with heating rate in pyrolysis. From **Fig.9(a)**, the yields of primary pyrolysis components, including benzene, styrene, indene, naphthalene, and PAHs (3–5 rings), rapidly increase with increase in the heating rate. The amount of aromatic hydrocarbons increases with increasing heating rate. The yields of toluene and xylene do not increase much with increase in the heating rate (**Fig. 9(b)**). On the other hand, at a slow heating rate the yields of straight-chain saturated hydrocarbons such as octane and phenol (OH group) increased. (**Fig.9(c)**) In addition to the above analysis, we investigated the molecular components and their structures of the tar by valuating FTIR (**Fig.10**: infrared absorption intensity data). Infrared absorption spectroscopy allows us to conduct qualitative and quantitative analyses of the functional groups present in the tar by observing the stretching and torsional behaviors of tar molecules. (The spectrometer has been used for analyzing asphalt and heavy oil [8].) In this study, IR spectrometer (IR μs spectrometer, Spectra-Tech Co. LTD, detection range: 4000–650 cm^{-1}; measurement mode: transmission method; resolution: 8 cm^{-1}; and accumulation number: 1024) was employed. The absorption peak in the vicinity of 3050 cm^{-1} is attributable to the C=C bonds or aromatic rings, and that in the vicinity of 2920 cm^{-1} is attributable to -CH_2- and -CH_3- groups. The peak in the vicinity of 1460 cm^{-1} is derived from the CH group. We evaluate the composition ratio of aromatic hydrocarbons including unsaturated aliphatic hydrocarbons to saturated aliphatic hydrocarbon in directly collected tar. Specifically, the change in the tar components with a heating rate ranging from 0.5 to 20 K/s was examined by determining the

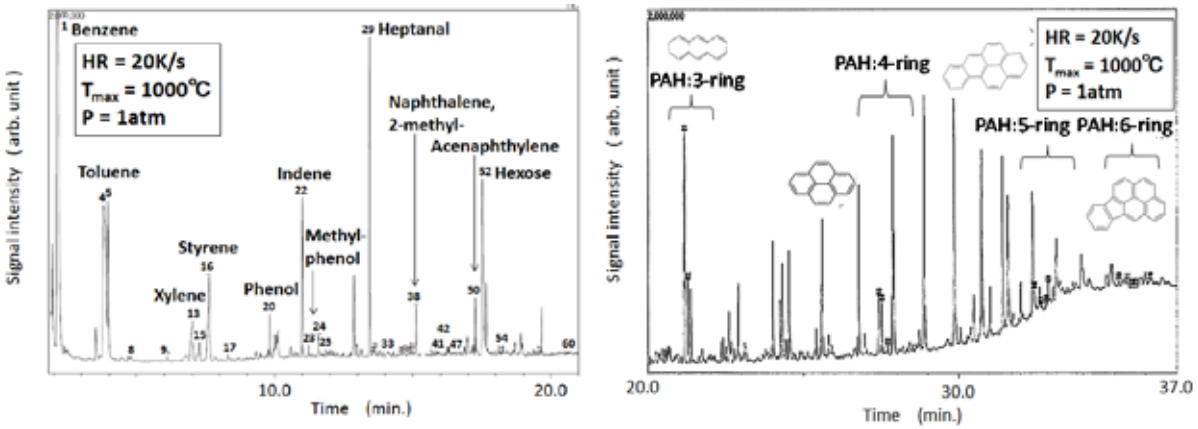

(a) Tar components at rapid heating rate detected by GC-MS (20K/s, 1atm)

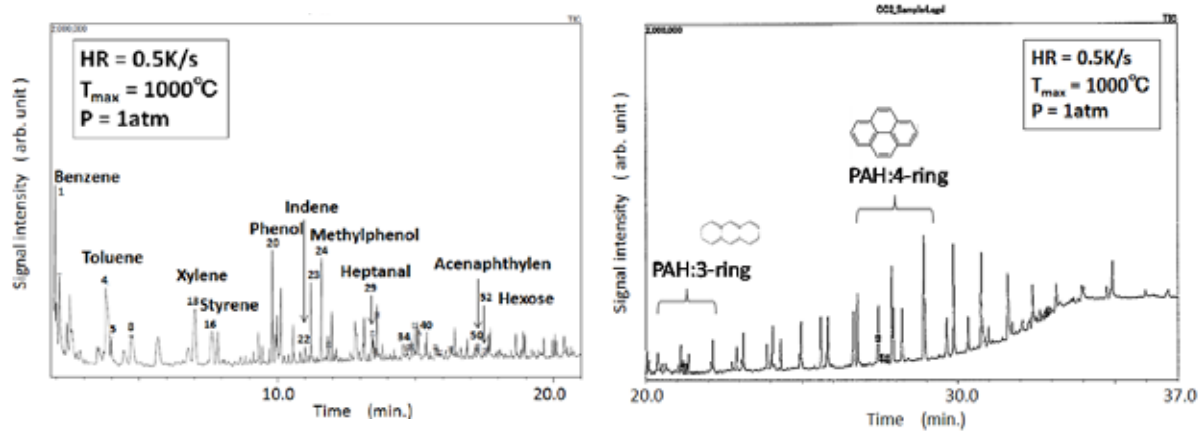

(b) Tar components at slow heating rate detected by GC-MS (0.5K/s, 1atm)

Fig.6 Effect of heating rate on first-pyrolysis product

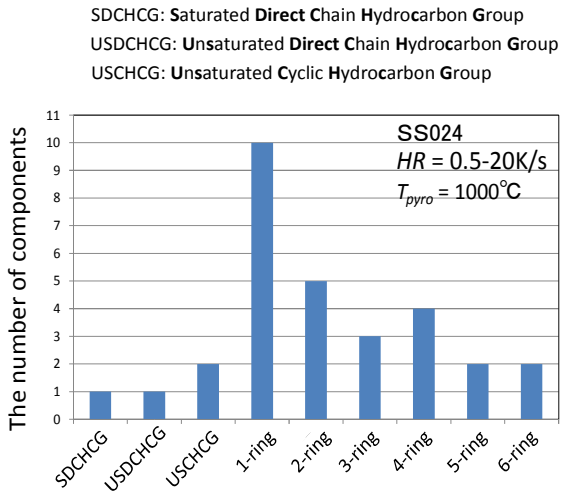

Fig. 7 Detected chemical species according to molecular configuration. (1atm)

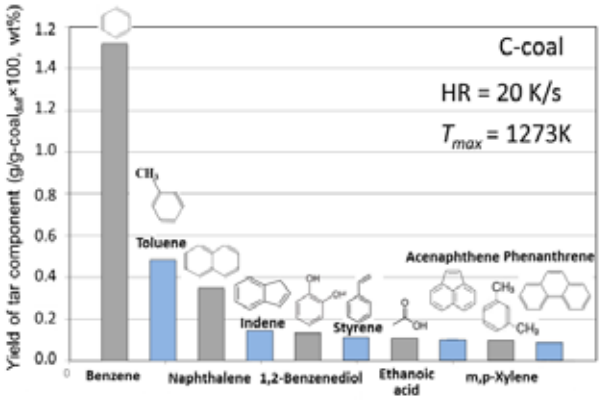

Fig. 8 Yield of major chemical species of pyrolysis tar. (5.0K/s, 1atm)

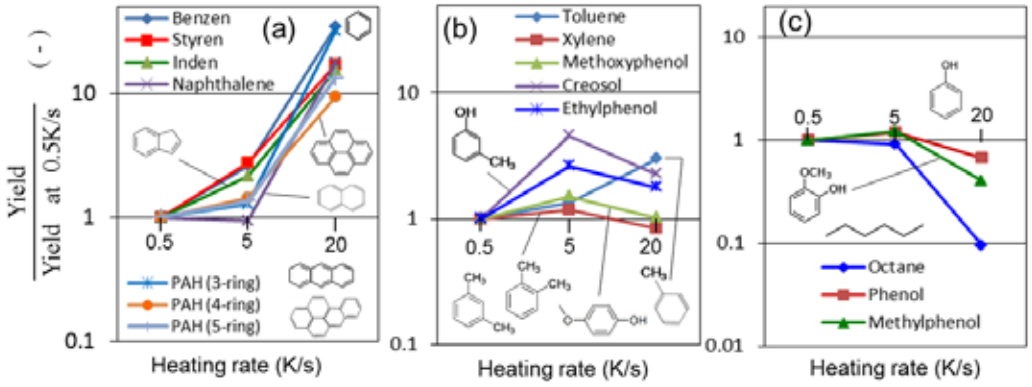

(a) increasing component (b) middle behavior (c) decreasing component

Fig.9 Effect of heating rate on tar-component yield (Coal type:SS024, Use in impinger, 1 atm)

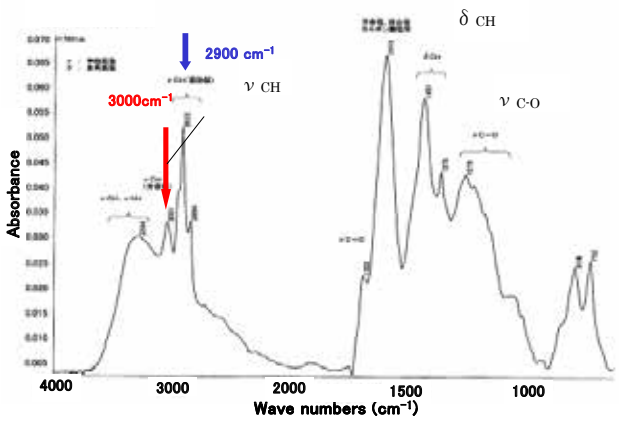

Fig.10 FTIR analysis of tar (20K/s, 1 atm)

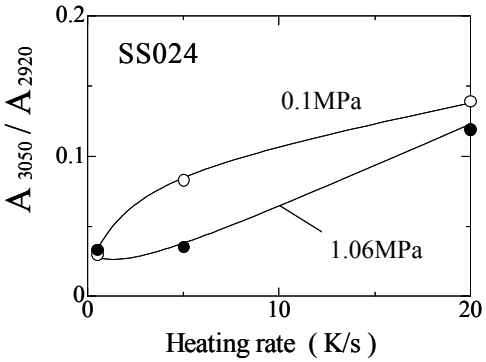

Fig.11 Effect of heating rate on molecule component of tar

integrated intensity ratio A_{3050}/A_{2920}. The higher the intensity ratio, the greater is the relative amount of aromatic hydrocarbons contained in tar components in the sample. **Figure 11** shows the dependence of the integral intensity ratio A_{3050}/A_{2920} on the heating rate. The results reveal that the relative amount of aromatic hydrocarbon components (i.e. polycyclic structures) tends to increase with increasing heating rate. A similar tendency was observed even under high pressure, although the effect observed under high pressure is smaller than that under atmospheric pressure.

2.2.3 Effect of coal type on tar component

We discuss the effect of coal type on the yields of tar components based on the pyrolysis experiment using 19 different coal types ranging from lignite to semi-anthracite coal. **Table 1** shows the properties of the coals used for these

experiments. A to H coals with different carbon contents (wt%) were used. Coals (1)-(3), I-III, and 1-2 were included for the specific reason that bituminous coal tar yields differ considerably depending on the coal type. Coals (1) and (3) were included for comparison with Coal D, as they have identical carbon contents. Similarly, Coal I-III was included for comparison with Coal F, and Coals 3 and 5 were included for allowing carbon content interpolation between Coals F and G, and between Coals G and H, respectively.

As a result, even when the carbon contents of the coals were almost the same, their yield of volatile matter were significantly different (**Fig.12**). Therefore, these yields need to be systematically organized using an indicative physical value. Here, we adopted the atomic ratio H/C for this purpose (**Fig.13**). We have shown that $Y_{total\ V.M.}$ and Y_{tar} in many coals can be predicted by determining the H/C ratio. In other words, $Y_{total\ V.M.}$ and Y_{tar} in many coals can be predicted by determining the H/C ratio. Below, we formulate predictive equations for the total volatile matter, and tar yields by applying the least-squares approximation to the yield data for various coals. (R shows the multiple correlation coefficient.)

$$Y_{total\ V.M} = 109\times(\mathrm{H/C}) - 47.0 \quad [\mathrm{wt\%}] \quad \cdots\cdot(5) \quad (R^2 = 0.837)$$

$$Y_{tar} = 30.4\times(\mathrm{H/C}) - 14.0 \quad [\mathrm{wt\%}] \quad \cdots\cdot(6) \quad (R^2 = 0.576)$$

Here, the yields of CH_4, C_2H_4, CO, CO_2, C_2H_4 (**Fig.14**) are shown as:

H_2 [wt%] : $Y_{H2} = 0.506\times(\mathrm{H/C}) + 1.73$ $\cdots\cdot$ (7) $(R^2 = 0.018)$

CH_4[wt%] : $Y_{CH4} = 6.63\times(\mathrm{H/C}) - 0.839$ $\cdots\cdot$ (8) $(R^2 = 0.611)$

CO[wt%] : $Y_{CO} = 75.6\times(\mathrm{O/C}) - 0.0284$ $\cdots\cdot$ (9) $(R^2 = 0.873)$

CO_2[wt%] : $Y_{CO2} = 39.7\times(\mathrm{O/C}) - 1.06$ $\cdots\cdot$(10) $(R^2 = 0.852)$

C_2H_4[wt%] : $Y_{C2H4} = 20.7\times(\mathrm{H/C}) - 12.0$ $\cdots\cdot$(11) $(R^2 = 0.641)$

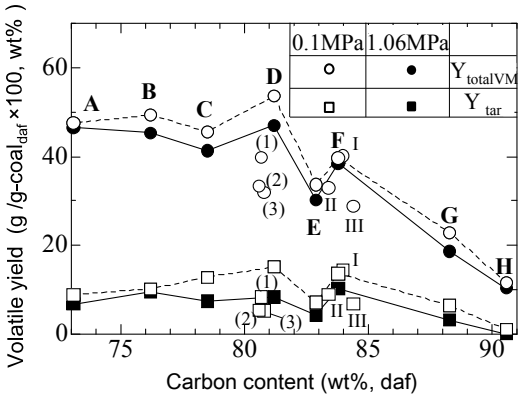

Fig.12 Effect of coal type on total yield of volatile matter and tar yield.

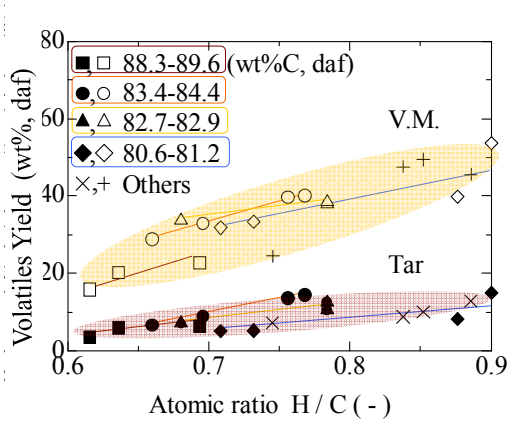

Fig.13 Changes in the volatile yields with atomic ratio H/C (1 atm)

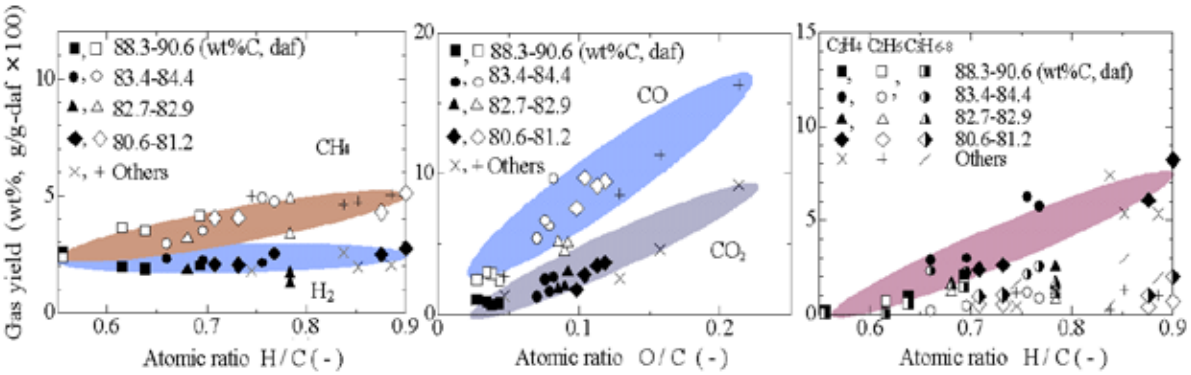

Fig.14 Dependence of gas yields on atomic ratio (20K/s, 1 atm)

M. Maroto-Valer et al.[9],[10] investigated more than 15 coal types using ^{13C} NMR (Carbon-13 Nuclear Magnetic Resonance) spectroscopy and suggested that the composition ratio of the aromatic compounds in each coal type decreases linearly with an increase in the H/C ratio. In the Progress DOE (United States Department of Energy) Report, Zilm et al.[11] suggested that the structure parameters of coals (i.e., the aliphatic-to-aromatic ratio) can be determined from the H/C ratio using ^{13C} NMR. Because the aliphatic-to-aromatic ratio can be determined using the H/C ratio [14], Y_{tar} could also be determined using the H/C ratio.

Figure 15 shows the effect of raw coal property on the yields of the functional tar components: benzene, toluene, and xylene (BTX). The yields of BTX components increased with increasing H/C ratio. In agreement with the results of **Fig. 13**, proportional increase of BTX components were observed.

Fig. 16 and **17** show the yields of two chemical raw materials, indene and fluorene, that can be used for advanced applications such as in medicines and resin modifiers[3] and as a functional raw material[4], respectively. As shown in **Fig. 16**, the yield of indene increases proportionally with the H/C ratio. However, as shown in **Fig.17**, that of fluorene increases considerably only for coals with a high H/C ratio. Furthermore, the yield of the normal chain saturated hydrocarbon, octane, shows a similar tendency. We revealed that both the yields of functional tar components increase for coal types with a high H/C ratio.

Finally, the yields of PAHs are discussed. Though not shown in figure, polycyclic aromatic components with 4- to 5-membered rings such as fluoranthene, dibenzo anthracene and benzopyrene etc. were observed, and polycyclic components with 6- or more-membered rings such as indenopyrene, and benzoperylene etc. were also observed. There is no correlation between H/C and PAHs yield (**Fig.18**) except in the case of polycyclic components with 3-membered ring (phenanthrene and anthracene

etc.), because the PAHs changes into soot and cokes (agglomerate components from liquid-tar to solid) are generated [12],[13].

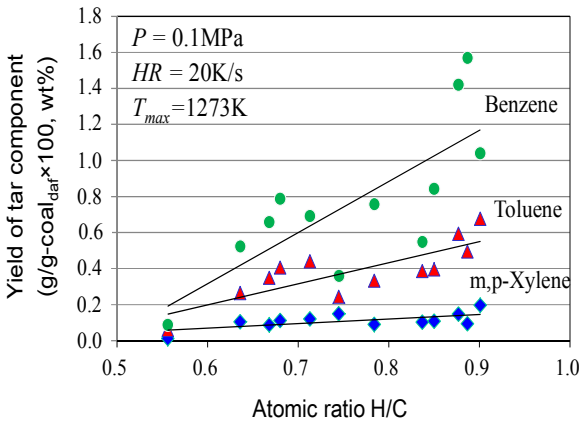

Fig.15 Effect of pressure on released volatile matter in various coal ranks (20K/s, 1 atm)

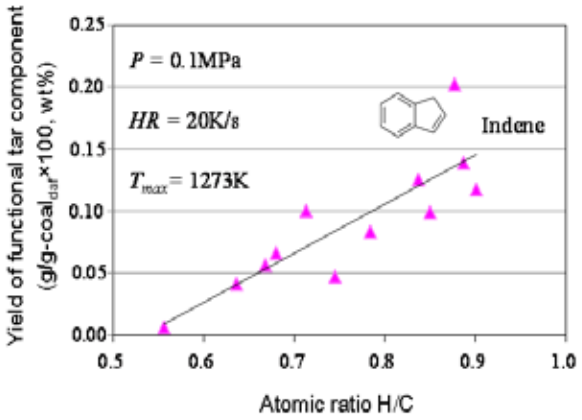

Fig.16 Effect of coal ranks on yield of indene
(for use in medicines and resin modifiers)

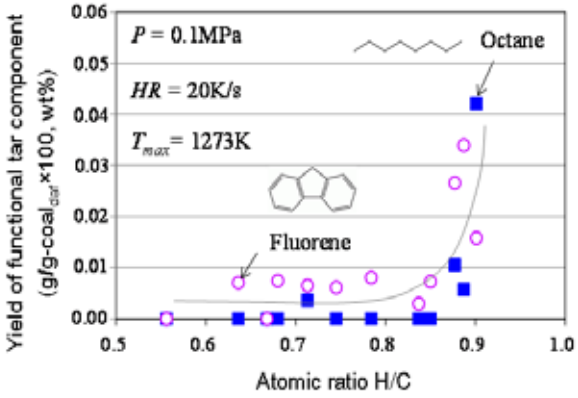

Fig.17 Effect of coal ranks on functional tar components
(Fluorene:for use in organic EL polymer skeletons, Octane: liquid fuel for engine)

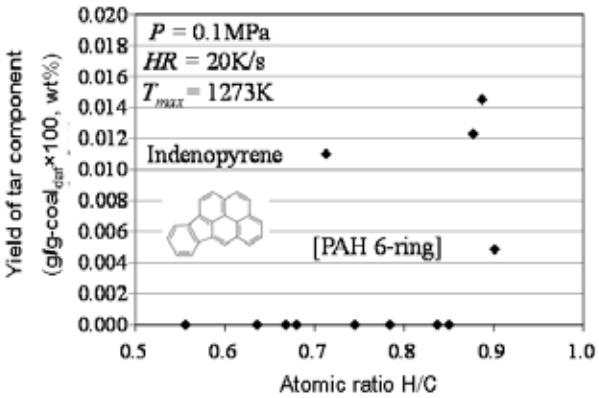

Fig.18 Effect of coal ranks on the yield of indenopyrene

As mentioned above, the variation in the yield with respect to an increased heating rate and the effect of coal type can be shown quantitatively in the research objective-(1).

3. RESEARCH OBJECTIVE-(2)

[Rapid Gasification of Biomass Feedstock at Low Temperatures]

3.1 Development of the Constituent Technologies

The rapid gasification of biochar at temperatures below approximately 600 °C is important to establish a system in which the by-product gas can be modified to a CO-rich gas and for which the FT synthesis is available using biomass at the temperature of the waste heat from a coke oven. However, the antagonistic conditions of low temperature and rapid gasification are difficult to attain simultaneously [14]. The pyrolysis rate of biomass is much faster than the gasification rate of char, and the overall conversion rate of biomass is controlled by the gasification reaction rate of char in the region of the endothermic reaction. For research objective-(2), a study to drastically increase the gasification reaction rate at low temperatures was performed with an alkali catalyst directly supported onto the char at 0, 2, 6, 10, or 20 wt%. The details of this study are described in the following section.

3.2 Experimental Apparatus and Method

(Preparation of biochar sample and gasification method)

The wheat straw (≒3.0 mm), rice straw(≒3.0 mm), rice husk, and Douglas-fir(1.0 - 4.0 mm) were used in this study. **Tables 3** and **4** show the results of ultimate and proximate analyses, respectively. The ash content increased in the order Douglas-fir chip < wheat straw < rice straw < rice husk (see **Table 4**). The chars were sifted to obtain samples with nearly same diameters and lengths. Chars were prepared with rapid heating rate in an argon environment. The pyrolysis conditions are shown in **Table 5**.

The chars produced by the pyrolysis process described in before were gasified using the thermobalance shown in **Fig. 2** (ALVAC 9600). The gasification kinetic rates of grass and woody biomass-derived char have been revealed by measuring the rate of weight loss during its reaction with CO_2 as a function of temperature (**Table 6**, 800/900/1000℃, 0.1MPa) [15],[16]. Gasification rate was determined using Eq. (8) based on the random pore model [17],[18].

Table 3 Ultimate analysis

	Ultimate analysis [daf wt%]					
	H/C	C	H	O	N	S
Douglas fir	1.31	52.10	5.70	42.10	0.10	0.006
Wheat straw	1.53	47.88	6.10	45.50	0.31	0.210
Rice straw	1.57	47.55	6.23	45.67	0.48	0.070
Rice husk	1.52	48.94	6.21	44.46	0.34	0.050

Table 4 Proximate analysis

	Proximate analysis [wt%]				
	HV (d.b.) [J/g]	VM	FC	Ash	Moist.
Douglas fir	19600	82.6	12.1	0.3	5.0
Wheat straw	17050	70.8	18.3	5.1	5.8
Rice straw	15520	65.5	16.6	11.1	6.8
Rice husk	14320	58.4	14.5	18.4	8.7

Table 5 Char-preparation experiment.

Exposure gas	Temp.(K)	Pressure(MPa)	Heating rate (K/s)	Holding time(min)
Ar	1073	0.1	10	0

Table 6 Gasification experiment

Gasification Temp (K)	Gasifing agent	Flow rate (ml/min)	Pressure (MPa)
1073, 1173, 1273	CO_2	400	0.1 (Atmospheric pressure)

$$\frac{dX}{dt} = K_p(1-X)\sqrt{1-\psi\ln(1-X)} \quad \cdots\cdots (8)$$

Solving Eq. (8) analytically, we obtain

$$X = 1 - \exp\left\{-K_p t\left(1 + \frac{\psi K_p t}{4}\right)\right\} \quad \cdots\cdots (9)$$

Transforming Eq. (9) and taking logarithms on both sides of the transformed equation, we rewrite Eq. (10) as

$$\frac{-\ln(1-X)}{t} = K_p + \frac{\psi K_p^{\,2}}{4} t \quad \cdots\cdots (10)$$

The gasification rate constant K_p and pore structure parameter ψ can be derived by determining the intercept and gradient of the straight line of $-\ln(1-X)/t$ versus t given by Eq. (10)

3.3 Method for directly supporting the catalyst on char samples

A catalyst (i) is supported on the raw biomass or (ii) is directly supported on the char. In general, a catalyst is supported on the raw biomass. However, a large amount of alkali metal (K, Ca, etc.) supported on the raw biomass may volatilize together with the pyrolysates during the pyrolysis reaction [19]. Therefore, we attempt to prevent the catalyst from scattering by adopting method (ii), above. Herein, we describe the direct method of supporting a catalyst on char. (This is new type of supporting method.) The raw biomass was pyrolyzed with conditions as described above. The raw biomass char sample was immersed in potassium acetate solution ($[CH_3COOK]_{aq}$ = 0.2 mol/L). The water present in the solution was evaporated at 105°C so that all the K components in the solution could be supported on the char [19].

(In a basic research, a raw biomass sample is immersed in a catalyst solution, as mentioned above. In an actual plant, char is isolated from the raw biomass and a catalyst solution is sprayed onto the isolated char). The weight ratio of char-supported K catalyst was calculated using next equation.

Weight ratio of char-supported K
= (weight of supported K) / (weight of char + weight of supported K) ···· (11)

Similarly, the biomass char sample was immersed in a 0.025-mol L-1 Fe(II) acetate solution (Fe(II) acetate; Wako. Co.). The water present in the solution was evaporated at 105°C so that all the Fe components in the solution could be supported on the char; this procedure is known as the evaporation drying method.

3.4 Experimental Results and Discussion

3.4.1 Effect of directly supported catalyst on rate-enhancement

The effect of a catalyst on the gasification rate is described below. From **Fig. 19**, the gasification rate of woody biomass can be improved remarkably by using potassium supported on char; a small amount of potassium (approximately 2 wt%) is sufficient to enhance the gasification of woody biomass char, which originally contains less ash, by three to four times or more. When the support ratio of K is 10 wt%, the rate-enhancement ratio is greater than 10. Here, the rate-enhancement ratio is calculated using the following equation: Rate enhancement = t/t_K
where t and t_K are the time required for carbon conversion from 0.0 to 1.0 for the raw biomass char and the K-supporting biomass char, respectively. In **Fig.20**, the

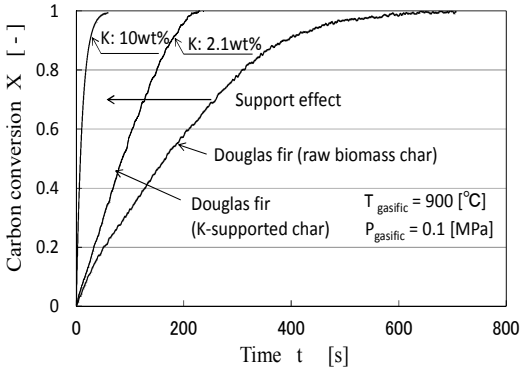

Fig.19 Effect of supported-K on carbon conversion rate
(Douglas-fir char: 900℃)

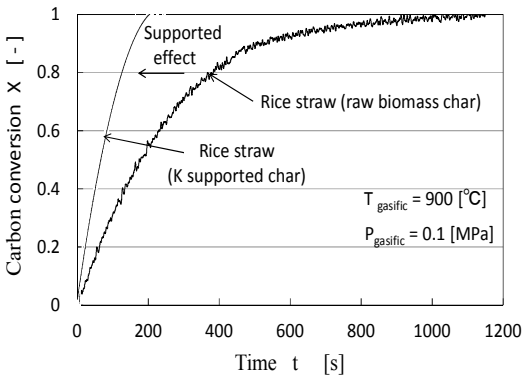

Fig.20 Effect of supported-K on gasification rate
(Rice straw char: 900℃)

variation in X with time is compared between raw and rice straw chars. It is clear that when the amount of supported K is approximately twice the ash content of raw biomass, the gasification time would be 1/5 times that in the case of raw char.

Figures 21 - 23 show the Arrhenius plots. The temperature dependence of gasification rate of K-supported chars indicates that the gasification can be activated over the whole measured temperature range. In addition, in the case of K-supported wheat straw char (**Fig.22**), rapid gasification (approximately $K_p \approx 0.1$/min) can be achieved at a low temperature of 650°C. From the viewpoint of the overall gasification process, the supported potassium significantly enhances the gasification rate; hence, the FT synthesis system can be downsized and the gasification conditions can be eased from higher temperature restriction.

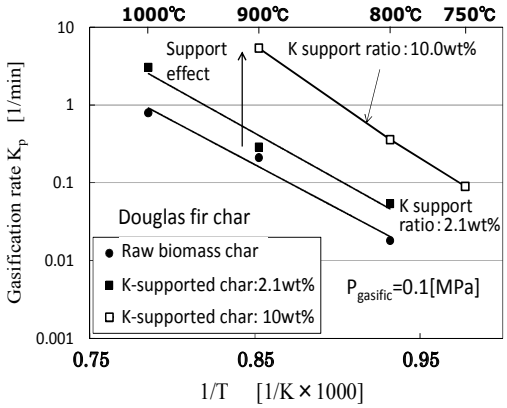

Fig.21 Effect of supported-K on gasification rate (Douglas-fir char)

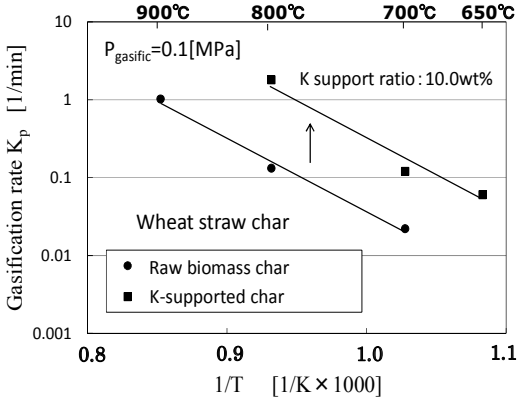

Fig.22 Effect of gasifying temperature on structure parameter (Wheat straw char)

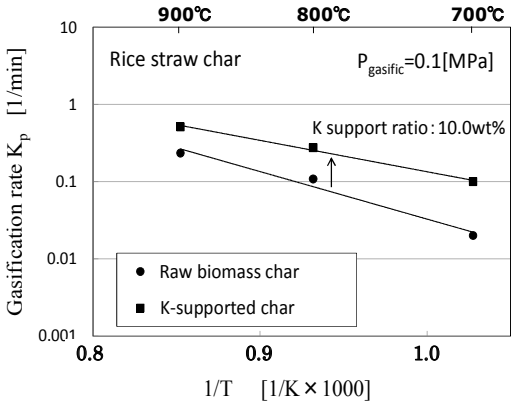

Fig.23 Effect of supported-K on gasification rate (Rice straw char)

As shown in **Fig. 21**, in the case of wooden biomass (Douglas fir), the rate constant for gasification of the biochar, K_p, with a small K-support ratio of 2.1 wt% was 1.5 - 4 times that of the raw biomass char. When the K-support ratio was 10 wt%, the value of K_p for the biochar was 20 - 25 times that of the raw biomass char. As seen in **Fig. 23**, the temperature dependence of gasification rate of K-supported rice straw char indicates an increase in the gasification rate owing to the catalyst with decreasing temperature and a decrease in the activation energy (i.e., the degree of slope).

3.4.2 Effect of the support ratio on rate-enhancement

Figures 24 and **25** show the gasification rates (Douglas-fir) of the K-supporting char and the Fe-supporting char, respectively. The gasification rate K_p of the catalyst-supporting char increased as the support ratio increased. The rate constant for gasification of the char on which 10 wt% of K was supported (K10) was approximately 300 times that of the deashed char (K0). However, when more than 10 wt% of K was supported, the gasification rate tended to be saturated. For the Fe-supporting char, although the gasification rate slightly increased as the support ratio increased, the gasification rate K_p of the char was markedly lower when Fe was supported than when K was supported. The gasification rates K_p of the char on which 23 wt% of Fe was supported (Fe23) at 900°C and 1000°C were approximately 3.3 and 10 times, respectively, that of the deashed char (Fe0). Comparing **Fig. 24** with **Fig. 25** revealed that the gasification rate of (K10) was approximately 90 times that of Fe10. Therefore, when K was directly supported on the char, the gasification rate at low temperatures could be drastically enhanced.

At present, the mechanism for the catalytic gasification has been elucidated based on the physical support morphology [22]. Here, the impregnation state of the catalyst in the char is investigated using a scanning electron microscope (i.e., cross-sectional analysis by EDS). Of course, there exist differences in this effect of each type of catalyst originally [20], [21].

For the K-supporting char, K was impregnated into the char, and the amount of K increased as the support ratio increased (not shown in the figure). Additionally, the crystal structure of K could not be confirmed. (I.e., in the char with a K-support ratio below 10 wt%, K was evenly distributed in the char. When the K-support ratio was above 20 wt%, K was locally concentrated in the char. There is a threshold value of K that must be supported on the char to achieve a homogeneous concentration.)

For the Fe-supporting char, Fe was difficult to impregnate into the char and that a large number of Fe crystals (α-FeOOH, α-Fe_2O_3) were laminated on the char surface.

For a char with a high support ratio, the excess supply of Fe on the char surface during the initial gasification stage decreased the number of active sites, which consisted of Fe and the char. Moreover, because the Fe crystals laminated on the char surface were easily detached from the surface as gasification advanced, the Fe catalyst could not function effectively.

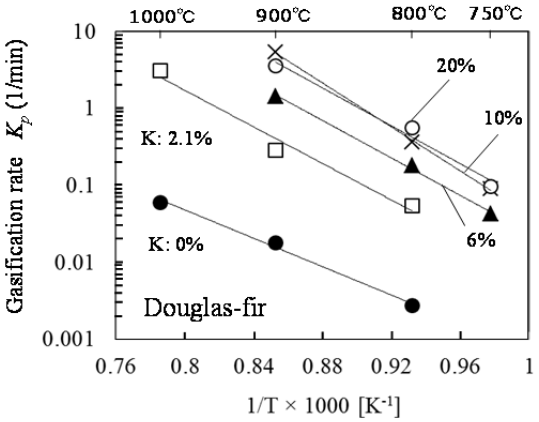

Fig.24 Effects of the Fe support ratio on the CO_2 gasification rate

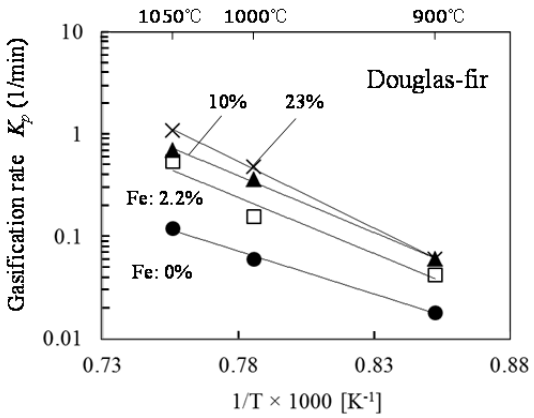

Fig.25 Effects of the K support ratio on the CO_2 gasification rate

4. CONCLUSION

The present study proposes a method to increase the yield of functional chemical raw materials in order to use in advanced chemical applications (research objective-(1)). Specifically, based on the results of (I) and (II) below, selecting a coal type with a high H/C ratio and performing fast pyrolysis for the selected coal were found to be important to obtain functional chemical raw materials. (I) The yields of the primary pyrolysis components such as benzene, styrene, indene, and naphthalene increase drastically with increasing heating rate. In addition, the yield of 3- to 6-membered-ring tar components (polycyclic aromatic hydrocarbons: PAHs) increases with increasing heating rate. (II) The tar yield increases linearly with the H/C ratio. Especially, the yield of indene, which can be used as a functional raw material, increased proportionally with increasing H/C ratio. Whereas, the yield of fluorene, which can be used to enhance resin functionality, increased only for coals with a high H/C ratio.

In the research objective-(2), this study aimed to realize the rapid gasification of biochar at low temperatures in order to produce liquid fuel from the by-product gas and biomass in the temperature range of waste heat. The experimental results show

that the high gasification rate of biomass char is appeared i.e., approximately 10 times higher than that of the raw biochar by directly supported catalyst. When using grass biochar on which potassium is directly supported, rapid gasification can be carried out at approximately 650°C. (When wheat straw is used, a gasification rate of $K_p \approx 0.1$/min can be achieved.)

ACKNOWLEDGMENT

This research was financially supported by the JFE 21st Century Foundation. The author is grateful to all those who have supported this study.

REFERENCE

[1] Schobert, H.H. et al., ***Fuel*** 81 (2002) 15–32.

[2] Li, C. et al., ***Resources, Conservation and Recycling*** 54 (2010) 905-915.

[3] ***Coal Science and Coal Technology***, Ed. Japan Institute of Energy, ISBN: 978-4-339- 06629-6, Corona Publishing Co. Ltd. (2013) 71-73.

[4] Dai Z. et al., ***European Polymer Journal*** 45 (2009) 1941–1948.

[5] Tanizawa K., "Establish SCOPE type new coke oven battery at NSSMC Nagoya works", ***Proc. the 52nd Conference on Coal Science, The Japan Institute of Energy*** (2015), ii-vii

[6] Cai H.-Y. et al., ***Fuel*** 75 (1996) 15-24.

[7] Gibbins-Matham J., Kandiyoti R., ***Energy Fuels*** 2 (1988) 505-511.

[8] Guillen M.D. et al., ***Fuel*** 74 (1995) 1595-1598.

[9] Maroto-Valer M. et al., ***Fuel*** 77 (1998) 783-785.

[10] Maroto-Valer M. et al., ***Fuel*** 77 (1998) 805-813.

[11] Zilm K., Advanced Solids NMR Studies of Coal Structure and Chemistry, ***Report No. DOE/PC/95227-5***, United States Department of Energy, 1998.

[12] Ledesma E.B. et al., ***Fuel*** 79 (2000) 1801-1814.

[13] Wijayanta A.T. et al., ***Fuel*** 93 (2012) 670-676.

[14] Hayashi J., ***Journal of Chemical Engineering of Japan (The Society of Chemical Engineers)***. Vol.76, No.4 (2012) , 190-192.

[15] Okumura Y., ***Journal of the Japan Institute of Energy***, Vol.90, No.2 (2011), 122-131.

[16] Okumura Y. et al., ***Proc. Combustion Institute***, Vol.32, Issue 2 (2009), 2013–2020.

[17] Bhatia S. K. et al., Carbon, Vol.34, Issue 11 (1996) 1383-1391.

[18] Zhang Y. et al., ***Fuel***, Vol.87 (2008), pp.475–481.

[19] Davidsson, K.O. et al., ***Fuel***, Vol.81 (2002) 137-142.

[20] Mitsuoka K. et al., ***Fuel Processing Technology***, Vol.92 (2011) 26–31.
[21] Huang Y. et al., ***Biotechnology advances***, Vol.27 (2009) 568-572.
[22] Okumura Y. et al., "A consideration on mechanism of enhancement of gasification rate of biomass char diagnosed by cross section of supported catalysts ", ***Proc. the 24th Annual Meeting of Japan Institute of Energy***, No.3-2-1 (2015), pp.72-73.
[23] Hanaoka T. et al., ***Journal of Thermal Science and Technology***, Vol.9, No.2 (2014), DOI: 10.1299/jtst.2014jtst0006.